Strain-tunable plasmonic crystal using elevated nanodisks with polarization-dependent characteristics

Yifei Wang,[1] Longju Liu,[1] Qiugu Wang,[1] Weikun Han,[1] Meng Lu,[1,2,a)] and Liang Dong[1,a)]
[1]*Department of Electrical and Computer Engineering, Iowa State University, Ames, Iowa 50011, USA*
[2]*Department of Mechanical Engineering, Iowa State University, Ames, Iowa 50011, USA*

(Received 19 November 2015; accepted 9 February 2016; published online 19 February 2016)

This paper reports on the mechanical tuning of optical resonances of a flexible plasmonic crystal. The device is structured with a square lattice nanopost array standing out of an elastomer substrate and coated with a gold thin film. The gold nanodisks residing on top of the nanoposts support a surface plasmon polariton (SPP) Bloch wave mode at the gold-air interface. By applying a strain along a planar direction of the substrate, the period of the elevated nanodisk array changes, thus altering the SPP resonance wavelength. Because the applied strain breaks period symmetry of the nanodisk array, the original single resonance mode is split into two polarized resonance modes. For the incident light polarized parallel with and perpendicular to the direction of the applied strain, the corresponding resonance modes are shifted in opposite directions at a rate of 1.6 ± 0.1 nm for every 1% change in strain. During stretching and compressing the substrate, the applied strains only change the period between nearby nanodisks without affecting their shape and morphology. This has improved reliability and repeatability of resonance tuning of the device. © *2016 AIP Publishing LLC*.
[http://dx.doi.org/10.1063/1.4942454]

Surface plasmons can concentrate optical fields as a result of oscillating surface charges at a metal/dielectric interface.[1] Many plasmonic nanostructures have been developed for various applications, including biochemical sensors, photodetectors, integrated optical components, and super-resolution imaging.[2,3] Recently, tunable plasmonics have attracted much attention,[4–7] as there is a need to adapt to changing application requirements by tuning the optical properties of plasmonic devices.[8] Of particular interest is to tune plasmonic resonance modes in metallic nanostructures, such as nanorods,[9] nanoholes,[10] nanoshells,[11] nanoparticles,[12] and nanorings.[13] Existing plasmonic resonance tuning methods include changing the material, geometrical, and structural properties of the nanostructures *via* optical, magnetic, electric, thermal, and mechanical means.[14–18] For example, electro-optical tuning uses phase transition materials, such as liquid crystal, to adjust environmental refractive index by electric field.[19] Magneto-optically active plasmonic nanoholes use ferromagnetic materials as device substrate.[20] Thermo-mechanical tuning has also been accomplished by moving bimetallic nanostructures on a silicon substrate by means of micro-electro-mechanical systems (MEMS) based cantilevers.[21] In recent years, a number of flexible electronic and photonic devices have been demonstrated by the use of stretchable substrates with low Young's modulus and high failure strain.[22,23] By creating an adjustable gap between nearby nanoparticles on the surface of an elastomer, mechanically tunable plasmonic nanostructures have also been developed.[24]

This paper reports a plasmonic crystal structure able to tune its optical resonance mode by applying mechanical strains. The device is formed by coating a gold thin film on the surface of a stretchable polydimethylsiloxane (PDMS) substrate containing a periodic array of polymer nanoposts with a square lattice. On top of the nanoposts there is an array of gold nanodisks. When a uniaxial strain is applied to the substrate along a planar direction, the period of the elevated nanodisk array will change, thus altering its plasmonic resonance wavelength. Because the applied uniaxial strain also breaks the period symmetry of the nanodisk array, the resonance modes for different polarizations of the incident light will be split and shifted in opposite directions. Thus, the polarization-dependent tuning of plasmonic spectra will be achieved. It is noteworthy that because the gold nanodisks are separated from the base substrate, applying strains to the substrate in any planar directions will not deform the gold nanodisks. This will allow for better control of plasmonic resonance and improve repeatability of resonance tuning.

Figure 1(a) shows the schematic for the plasmonic device with an array of gold-coated nanoposts. The resonance wavelength λ of the structure can be approximately calculated by the equation:[25] $\lambda = \frac{\Lambda}{\sqrt{i^2+j^2}}\sqrt{\frac{\varepsilon_{Au}\varepsilon_d}{\varepsilon_{Au}+\varepsilon_d}}$, where ε_{Au} and ε_d represent the permittivity of gold and free space, respectively, and i and j are the order of surface plasmon polariton (SPP) Bloch wave. The Young's modulus E of the PDMS substrate can be calculated by dividing the stress by the average stain, which is given by $E = FL_0/A_0\Delta L$, where F is the normal component force exerted on the stress area A_0, L_0 is the initial length of the PDMS substrate, and ΔL is the change of its length. The strain $\varepsilon = \Delta L/L_0 = \Delta\Lambda/\Lambda$ represents the percentage of the overall deformation. When an outward force is applied to the substrate in a planar direction, the period of the nanopost array in the same direction will increase by $\Delta\Lambda$, while in the orthogonal direction of the same plane the period will decrease by the same amount (upper panel in Figure 1(b)). Therefore, the gold nanodisks will gain

a)Authors to whom correspondence should be addressed. Electronic addresses: ldong@iastate.edu and menglu@iastate.edu

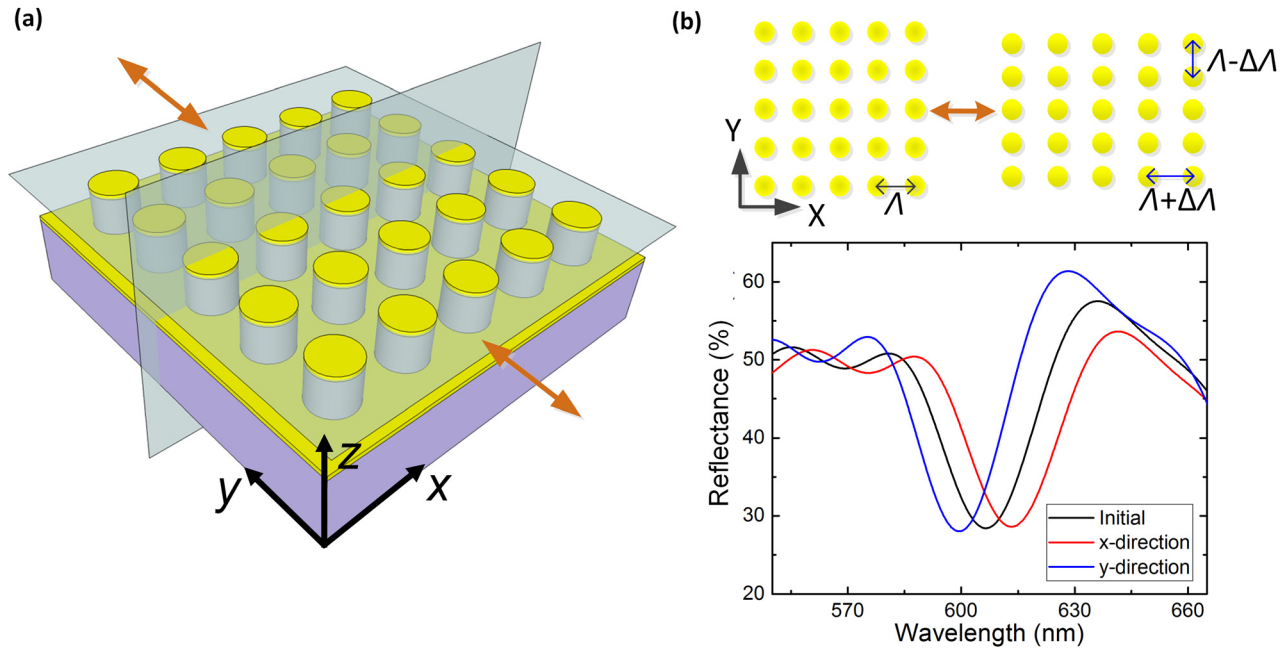

FIG. 1. (a) Schematic of the tunable plasmonic crystal using elevated gold nanodisks. (b) Simulated reflection spectra of the device showing that a strain applied along the *x*-direction introduces opposite dimensional changes in two directions of the square lattice. The original single resonance mode is split into two resonance modes for the incident light polarized along two directions.

asymmetry in period between the two planar directions, accompanied by changing the shape of the substrate. As a result, there will be two plasmonic modes present with regard to the different polarizations of the excitation light (lower panel in Figure 1(b)). Specifically, when the PDMS substrate is stretched along the *y*-direction (*x*-direction), the incident light polarized along the *y*-direction (*x*-direction) will excite a plasmonic resonance at a longer wavelength, while for the incident light polarized in the *x*-direction (*y*-direction), the excited resonance will appear at a shorter wavelength. Furthermore, by applying different strains along either direction, the *x*- and the *y*-polarized resonance wavelengths will be shifted in the opposite directions. Therefore, mechanical tuning of the plasmon resonance wavelengths will be achieved, along with the polarization-dependent feature.

Full wave electromagnetic simulations, based on a finite different time domain method, was used to study optical responses of the device with the lattice period of $\Lambda = 600$ nm, the post diameter of $d = 195$ nm, the post height of $h = 250$ nm, and the gold thickness of 50 nm. The details of the optical simulation are described in the supplementary material.[26] Figure 1(b) shows that when the elastomer substrate is not stressed, the simulated original resonance occurs at the wavelength of 607 nm. When the device is stretched along the *x*-direction by 5%, the *x*- and *y*-polarized resonances are shifted to 613.3 nm and 599.5 nm, respectively. Figures 2(a) and 2(b) show the simulated electric field intensity distribution at 607 nm when the substrate is not stressed. The result indicates that the resonance mode is confined mainly at the elevated nanodisks but only a little at the bottom of the nanoposts.

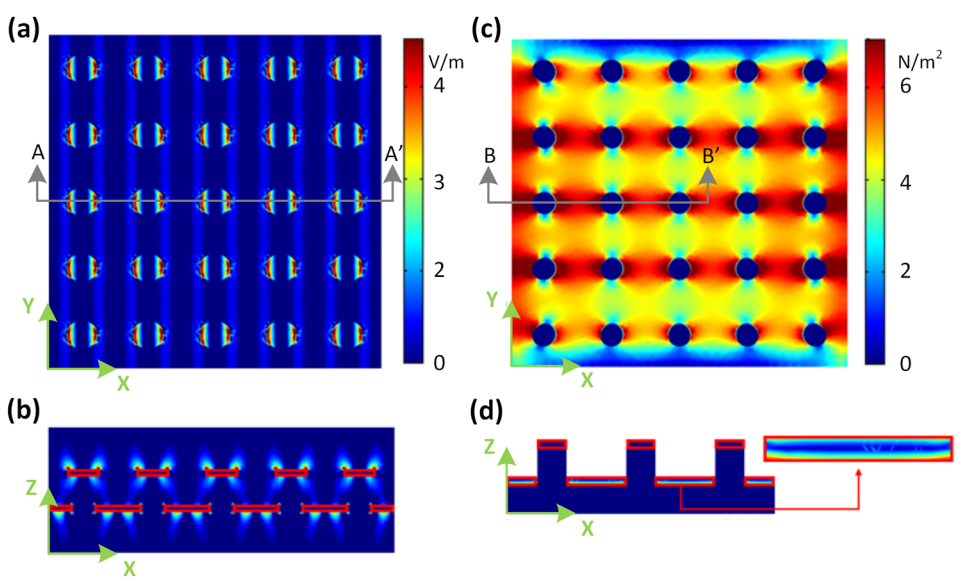

FIG. 2. (a) and (b) Top view and cross-section view (at A-A′) of the simulated electric field intensity distribution at the original resonance mode of $\lambda = 607$ nm. (c) and (d) Top view and cross-section view (at B-B′) of the simulated surface stress distribution.

Figures 2(c) and 2(d) illustrate the surface stress distribution on the surface of the whole device simulated using a finite element method based software COMSOL. When a tensile strength of 700 kPa is applied to the two sides of the substrate along the *x*-direction, high surface stresses are generated in the surface between the nanoposts but zero stress at the elevated gold nanodisks. The shape of the nanodisks is thus not affected. This feature, in conjunction with the fact that the resonance mode is mainly confined at the nanodisks, will make the resonance tuning more controllable with better repeatability, particularly as the resonance mode is majorly determined by the period of the nanodisks rather than their shape and dimensions. Note that the fabricated device has a 2 mm thick PDMS substrate. Limited by computational power, a reduced model with 200 nm thick PDMS substrate was calculated for illustrating the stress distribution on the surface of the device. The validation of the reduced model used in the mechanical simulation is described in the supplementary material.[26]

The proposed device was fabricated using a soft lithography-based nanoreplica molding process. The details of fabrication are described in the supplementary material.[26] Briefly, the fabrication involved two sequential replication steps as shown in Figures 3(a)–3(f). First, a silicon master mold carrying a positive surface structure of the nanopost array was used to create a soft PDMS mold with a negative surface profile of the finished device (Figures 3(a)–3(c)). Subsequently, the soft mold was used to form the PDMS nanoposts with the features identical to those on the silicon stamp (Figures 3(d) and 3(e)). After the two-step replications, a 50 nm thick gold film was evaporated on the whole surface of the device (Figure 3(f)). The size of the device is 8 mm (width) × 8 mm (length) × 2 mm (thickness). Figure 2(g) shows a scanning electron microscope (SEM) image of the fabricated device.

The reflection spectra of the fabricated device at different stretching and compression ratios were measured. The details of the optical and mechanical measurement setup are shown in supplementary material.[26] The testing spot (2 mm diameter) locates at the center of the device, where the lateral stress is relatively uniform. Figure 3(h) shows that when no strain is applied, the resonance wavelength is measured to be 600.2 nm. Because of the initial square lattice arrangement, the resonance wavelength of the device is independent of polarization of the

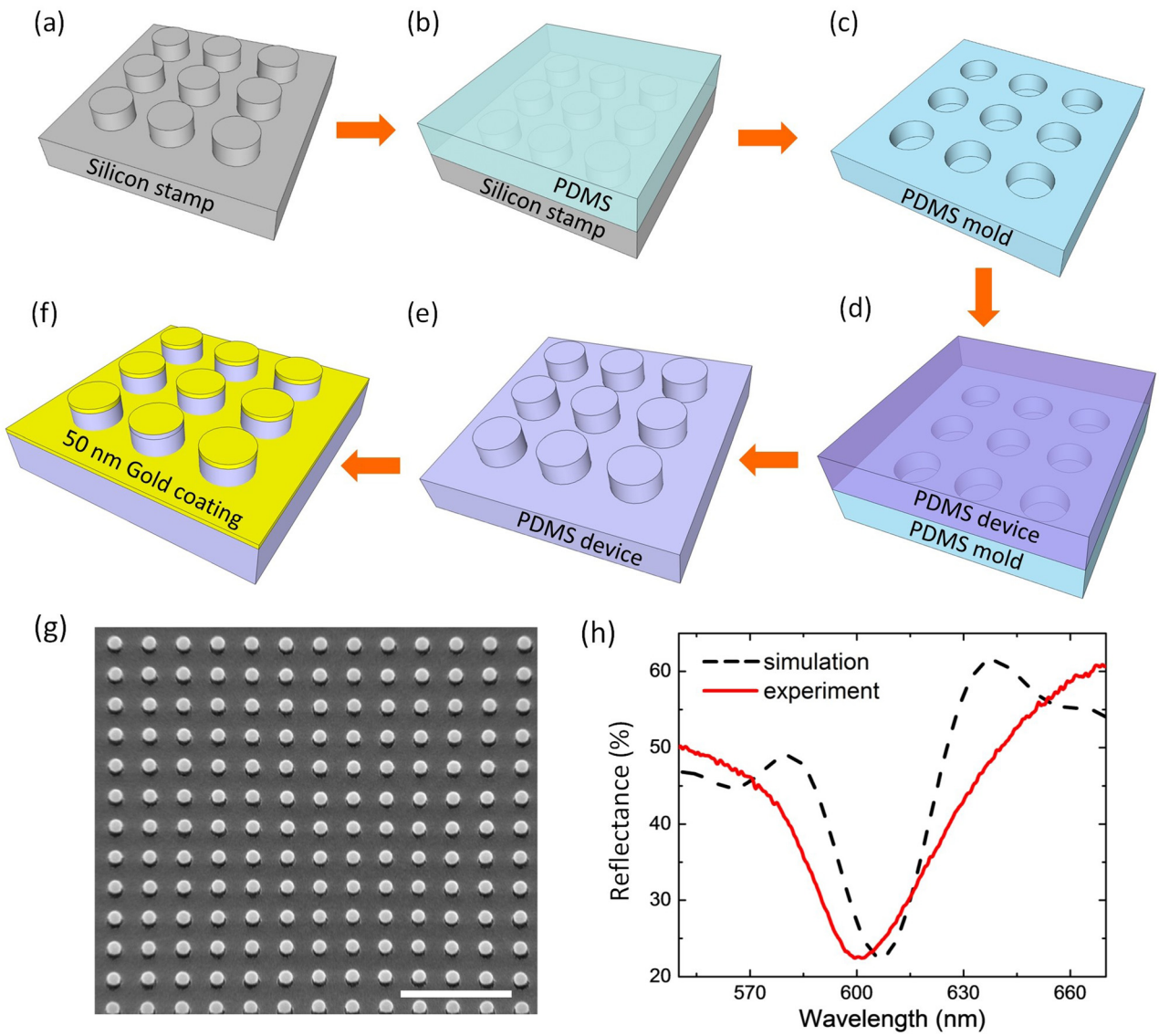

FIG. 3. (a)–(f) Schematic of the fabrication process. (g) An SEM image of the device. Scale bar: 2 μm. (h) Measured reflection spectrum of the nanostructure without any applied strain. For the purpose of comparison, the simulated reflection spectrum is plotted as a dashed line.

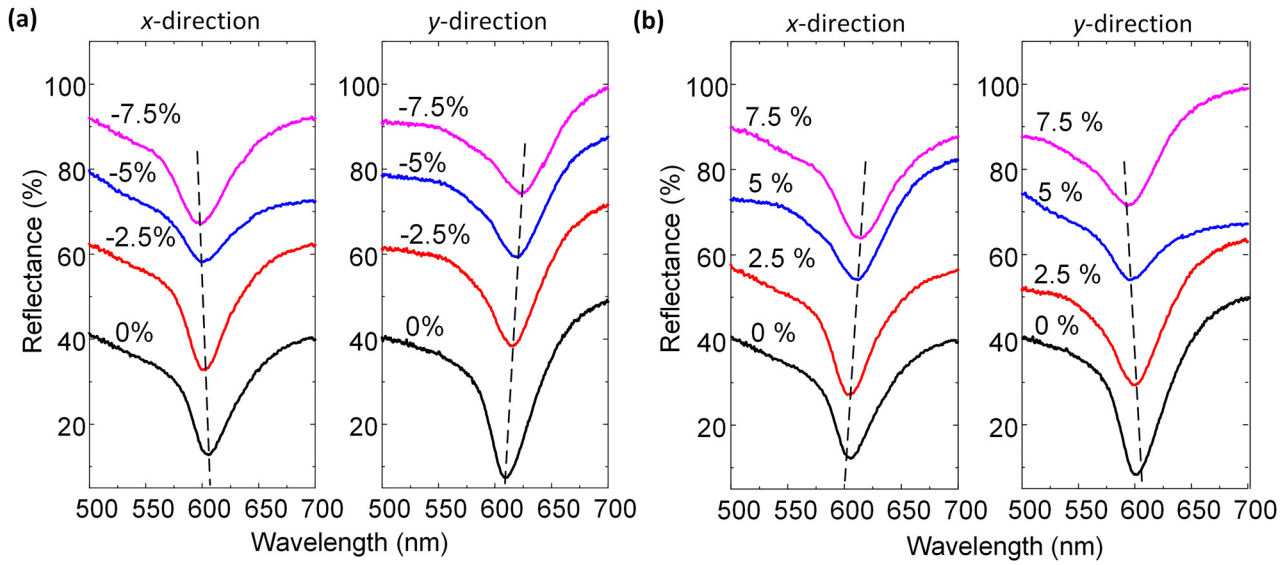

FIG. 4. Measured reflection spectra of the plasmonic nanostructure with different compressive (a) and tensile (b) strains for the incident light polarized along the *x*-direction (left panel) and the *y*-direction (right panel).

excitation light. Figure 4(a) shows the reflection spectra of the device when responding to different compressive strains (0, −2.5%, −5%, and −7.5%) applied to the substrate along the *x*-direction. As the strain further increased, the resonance spectrum would keep shifting but the bandwidth would start to increase. The incident light was polarized along the *x*- and *y*-direction. As is apparent from the plot, as the compressive strain increases, the *x*-polarized resonance mode is shifted towards shorter wavelengths, while the *y*-polarized one is shifted toward longer wavelengths. As expected, when the tensile strain along the *x*-direction increases (Figure 4(b)), the *x*- and *y*-polarized modes are shifted towards longer and shorter wavelengths, respectively.

Figure 5 summarizes the resonance wavelengths of the device as a function of applied compressive and tensile strains. Here, the PDMS substrate was stretched or compressed along the *x*-direction by an incremental strain of 0.25%. The strain was cumulatively loaded to the sample without being released to the original state before applying a higher strain. The result indicates that in the case of compression (Figure 5(a)), the *x*- and *y*-polarized resonance wavelengths almost linearly decrease and increase with the applied strains, respectively. By fitting the response curves with a linear function, the resonance sensitivity to a change in negative strain with the incident light polarized in the *x*- and *y*-direction is obtained to be 1.6 and 1.59 nm per 1% change in strain, respectively. In the case of stretching (Figure 5(b)), the *x*- and *y*-polarized resonances also respond linearly to changing strains, but with an opposite changing tendency to that shown in the case of compression. The sensitivity of the *x*- and *y*-polarized resonance to strain is 1.62 nm and 1.61 nm per 1% change in strain, respectively.

The previously reported strain-tunable metamaterials based on split ring resonators are able to tune their resonant wavelength by ∼7 nm for every 1% change in applied strain.[4] But, it should be pointed out that these plasmonic structures operate in the mid infrared (IR) regime centered at $\lambda_c \approx 3.75\ \mu$m. By taking into account this operating wavelength, their resonance sensitivity to strain normalized by λ_c is only 0.00186 per 1% change in strain. Another strain-tunable plasmonic structure composed of a monolayer array of gold semishells with dielectric cores shows the spectrum tuning of ∼3.5 nm per 1% change in strain in the near IR region centered at $\lambda_c \approx 1.55\ \mu$m.[14] Thus, the normalized resonance sensitivity to strain for the structure is 0.00226 for every 1% change in strain. In comparison, as mentioned earlier, our plasmonic crystal resonates at the wavelength of 600.2 nm when no strain is applied. The normalized sensitivity of the *x*- and *y*-polarized resonance of our device to applied strain can be calculated as 0.0027 and 0.00268 per 1% change in strain, respectively. Therefore, the

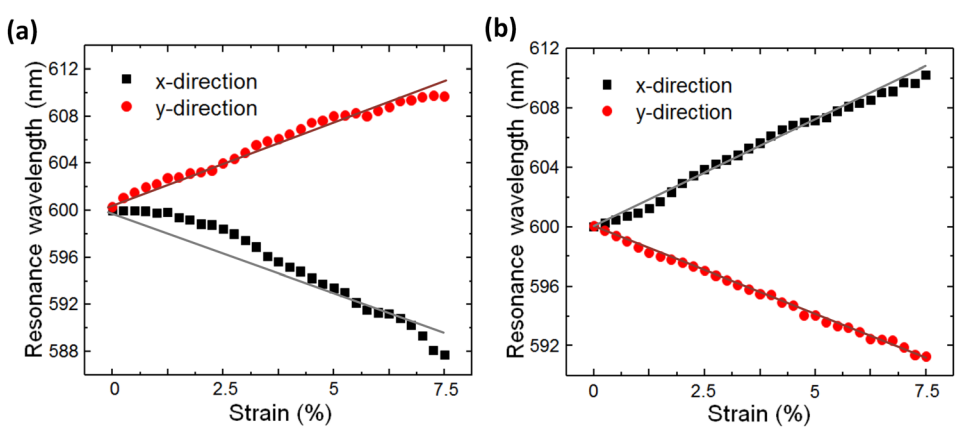

FIG. 5. Continuous tuning of the plasmon resonance by applying compressive (a) and tensile (b) strains along the y-direction of the PDMS substrate. Incident light was polarized along the *x*-direction (black squares) and *y*-direction (red dots).

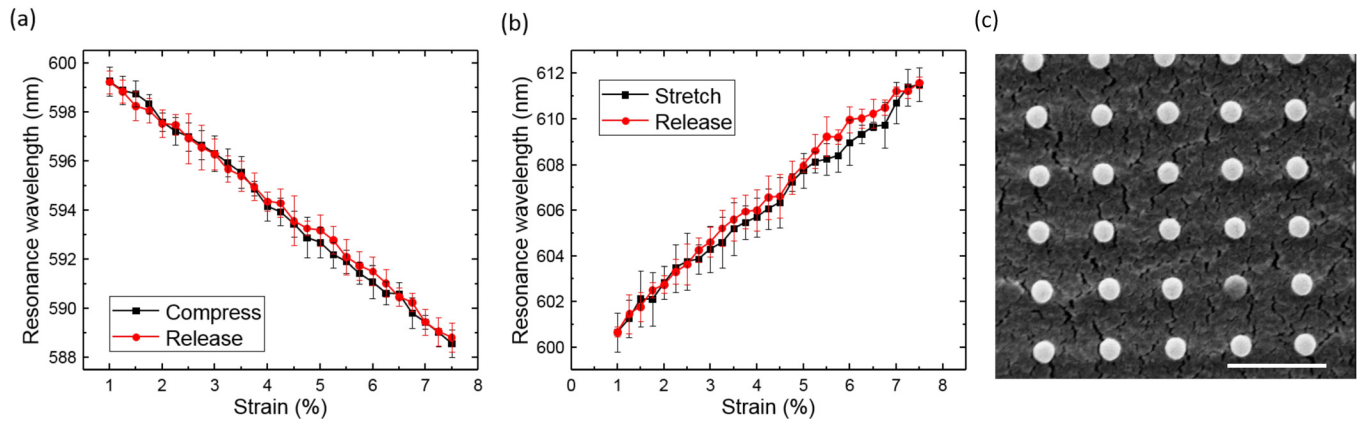

FIG. 6. (a) and (b) Repeatability test of resonance tuning by cyclic compression-release (a) and stretch-release (b) tests for 1000 times. (c) SEM image of the device when compressed at 5% strain after the cyclic stretch-release and compression-release tests. Scale bar presents 1 μm.

tuning performance of our device is reasonable and competitive compared with other tunable plasmonic devices.[4,14]

We tested repeatability of resonance tuning by stressing the substrate for multiple cycles. For each cyclic compression/stretching measurement, after the substrate was stressed in the *x*-direction and the resonance wavelength was recorded, it retraced back to the initial unstressed state to complete one cycle. The incident light used here was polarized in the *x*-direction. Figures 6(a) and 6(b) show the results from 1000 cycles each for the compression and stretching tests. It is demonstrated that the device has a high operation repeatability of tuning its plasmonic resonance. Figure 6(c) shows the SEM image of the device in the compressed state with 5% strain applied after 1000-cycle stretch-release and 1000-cycle compression-release tests. While the gold film between the nanoposts on the substrate has shown a few cracks after the cyclic measurement, the gold nanodisks are still intact without any damage. It is believed that the obtained good repeatability of resonance tuning is attributed to these damage-free gold nanodisks that are critical to the resonance mode majorly confined at the nanodisks.

In summary, we have demonstrated a strain-tunable plasmonic crystal consisting of an array of gold nanodisks elevated from the base surface of an elastomer substrate. During stretching and compressing the substrate, the nanodisks are not mechanically influenced, while their period is changed. This design has improved the tuning controllability and repeatability of the device. We have also demonstrated that applying in-plane strain along a primary direction results in the period asymmetry of the gold nanodisks between two planar directions of the square lattice, and thus, the original resonance mode is split into two resonance modes for the incident light polarized in the two directions. The present plasmonic crystal offers a reliable scheme of tuning optical resonance. The strain-induced polarization-dependent resonance tuning may find applications in optical filters, mechanical sensors, and biochemical sensors. Future work includes applying this tuning mechanism to other plasmonic crystal structures with different pattern size, period, and lattice.

This research was supported in part by the new faculty start-up funds from the Iowa State University, National Science Foundation through the grant number ECCS-0954765, and Iowa Department of Transportation. Y.W. acknowledges financial support through M.L.'s Northrop Grumman professorship.

[1]W. L. Barnes, A. Dereux, and T. W. Ebbesen, Nature **424**, 824 (2003).
[2]J. Homola, Chem. Rev. **108**, 462 (2008).
[3]M. W. Knight, H. Sobhani, P. Nordlander, and N. J. Halas, Science **332**, 702 (2011).
[4]I. M. Pryce, K. Aydin, Y. A. Kelaita, R. M. Briggs, and H. A. Atwater, Nano Lett. **10**, 4222 (2010).
[5]I. M. Pryce, K. Aydin, Y. A. Kelaita, R. M. Briggs, and H. A. Atwater, Philos. Trans. R. Soc. A. **369**, 3447 (2011).
[6]J. Ding, B. Arigong, H. Ren, M. Zhou, J. Shao, M. Lu, Y. Chai, Y. Lin, and H. Zhang, Sci. Rep. **4**, 6128 (2014).
[7]J.-Y. Ou, E. Plum, J. Zhang, and N. I. Zheludev, Nat. Nanotechnol. **8**, 252 (2013).
[8]S. Lee, S. Kim, T.-T. Kim, Y. Kim, M. Choi, S. H. Lee, J.-Y. Kim, and B. Min, Adv. Mater. **24**, 3491 (2012).
[9]A. V. Kabashin, P. Evans, S. Pastkovsky, W. Hendren, G. A. Wurtz, R. Atkinson, R. Pollard, V. A. Podolskiy, and A. V. Zayats, Nat. Mater. **8**, 867 (2009).
[10]M. R. Gartia, A. Hsiao, A. Pokhriyal, S. Seo, G. Kulsharova, B. T. Cunningham, T. C. Bond, and G. L. Liu, Adv. Opt. Mater. **1**, 68 (2013).
[11]H. Wang, J. Kundu, and N. J. Halas, Angew. Chem. Int. Ed. **46**, 9040 (2007).
[12]Y.-L. Chiang, C.-W. Chen, C.-H. Wang, C.-Y. Hsieh, Y.-T. Chen, H.-Y. Shih, and Y.-F. Chen, Appl. Phys. Lett. **96**, 041904 (2010).
[13]E. M. Larsson, J. Alegret, M. Kall, and D. S. Sutherland, Nano Lett. **7**, 1256 (2007).
[14]X. Zhu, S. Xiao, L. Shi, X. Liu, J. Zi, O. Hansen, and N. A. Mortensen, Opt. Express **20**, 5237 (2012).
[15]X. Zhang, B. Sun, J. M. Hodgkiss, and R. H. Friend, Adv. Mater. **20**, 4455 (2008).
[16]W. Dickson, G. A. Wurtz, P. R. Evans, R. J. Pollard, and A. V. Zayats, Nano Lett. **8**, 281 (2008).
[17]G. Xu, C.-M. Huang, P. Jin, M. Tazawa, and D.-M. Chen, J. Appl. Phys. **104**, 053101 (2008).
[18]X. Zhu, L. Shi, X. Liu, J. Zi, and Z. Wang, Nano Res. **3**, 807 (2010).
[19]P. A. Kossyrev, A. J. Yin, S. G. Cloutier, D. A. Cardimona, D. H. Huang, P. M. Alsing, and J. M. Xu, Nano Lett. **5**, 1978 (2005).
[20]E. T. Papaioannou, V. Kapaklis, P. Patoka, M. Giersig, P. Fumagalli, A. Garcia-Martin, E. Ferreiro-Vila, and G. Ctistis, Phys. Rev. B **81**, 054424 (2010).
[21]M. A. Kats, R. Blanchard, P. Genevet, Z. Yang, M. M. Qazilbash, D. N. Basov, S. Ramanathan, and F. Capasso, Opt. Lett. **38**, 368 (2013).
[22]D.-H. Kim, N. Lu, Y. Huang, and J. A. Rogers, MRS Bull. **37**, 226 (2012).
[23]P. Liu, S. Yang, A. Jain, Q. Wang, H. Jiang, J. Song, T. Koschny, C. M. Soukoulis, and L. Dong, J. Appl. Phys. **118**, 014504 (2015).
[24]W. Song, A. E. Vasdekis, and D. Psaltis, Lab Chip **12**, 3590 (2012).
[25]H. F. Ghaemi, T. Thio, D. E. Grupp, T. W. Ebbesen, and H. J. Lezec, Phys. Rev. B **58**, 6779 (1998).
[26]See supplementary material at http://dx.doi.org/10.1063/1.4942454 for electromagnetic and mechanical simulations, microfabrication, and measurement methods.